**Title:** The effect of warming on grassland evapotranspiration partitioning using laser-based isotope monitoring techniques

**Running title:** Warming effect on ET partition

**Article type:** Special Issue of "Hydrogen isotopes as environmental recorders"

**Authors:** Lixin Wang[1,2], Shuli Niu[3], Stephen P. Good[4], Keir Soderberg[4], Matthew F. McCabe[2,5], Rebecca A. Sherry[3], Yiqi Luo[3], Xuhui Zhou[6], Jianyang Xia[3], Kelly K. Caylor[4]

1. Department of Earth Sciences, Indiana University-Purdue University, Indianapolis (IUPUI), Indianapolis, Indiana 46202, USA

2. Water Research Center, School of Civil and Environmental Engineering, University of New South Wales, Sydney, NSW, 2052, Australia

3. Department of Botany and Microbiology, University of Oklahoma, Norman, OK 73019, USA

4. Department of Civil and Environmental Engineering, Princeton University, Princeton, NJ, 08544, USA

5. Water Desalination and Reuse Center, King Abdullah University of Science and Technology, Thuwal, Saudi Arabia

6. Research Institute for the Changing Global Environment, Fudan University, 220 Handan Road, Shanghai, 200433, China

Date of the revised manuscript draft: December 18, 2012
Manuscript word count (including text, references and figure captions): 7405

*Corresponding author

Lixin Wang
Department of Earth Sciences
Indiana University-Purdue University, Indianapolis (IUPUI)
Indianapolis, Indiana 46202, USA
E-mail: w.lixin@gmail.com
Telephone: 434-260-1090

This is the author's manuscript of the article published in final edited form as:
Wang, L., Niu, S., Good, S. P., Soderberg, K., McCabe, M. F., Sherry, R. A., ... & Caylor, K. K. (2013). The effect of warming on grassland evapotranspiration partitioning using laser-based isotope monitoring techniques. Geochimica et Cosmochimica Acta, 111, 28-38.
http://dx.doi.org/10.1016/j.gca.2012.12.047

**Abstract**

The proportion of transpiration (*T*) in total evapotranspiration (*ET*) is an important parameter that provides insight into the degree of biological influence on the hydrological cycles. Studies addressing the effects of climatic warming on the ecosystem total water balance are scarce, and measured warming effects on the *T/ET* ratio in field experiments have not been seen in the literature. In this study, we quantified *T/ET* ratios under ambient and warming treatments in a grassland ecosystem using a stable isotope approach. The measurements were made at a long-term grassland warming site in Oklahoma during the May-June peak growing season of 2011. Chamber-based methods were used to estimate the $\delta^2$H isotopic composition of evaporation ($\delta_E$), transpiration ($\delta_T$) and the aggregated evapotranspiration ($\delta_{ET}$). A modified commercial conifer leaf chamber was used for $\delta_T$, a modified commercial soil chamber was used for $\delta_E$ and a custom built chamber was used for $\delta_{ET}$. The $\delta_E$, $\delta_{ET}$ and $\delta_T$ were quantified using both the Keeling plot approach and a mass balance method, with the Craig-Gordon model approach also used to calculate $\delta_E$. Multiple methods demonstrated no significant difference between control and warming plots for both $\delta_{ET}$ and $\delta_T$. Though the chamber-based estimates and the Craig-Gordon results diverged by about 12‰, all methods showed that $\delta_E$ was more depleted in the warming plots. This decrease in $\delta_E$ indicates that the evaporation flux as a percentage of total water flux necessarily decreased for $\delta_{ET}$ to remain constant, which was confirmed by field observations. The *T/ET* ratio in the control treatment was 0.65 or 0.77 and the ratio found in the warming treatment was 0.83 or 0.86, based on the chamber method and the Craig-Gordon approach. Sensitivity analysis of the Craig-Gordon model demonstrates that the warming-induced decrease in

soil liquid water isotopic composition is the major factor responsible for the observed $\delta_E$ depletion and the temperature dependent equilibrium effects are minor. Multiple lines of evidence indicate that the increased *T/ET* ratio under warming is caused mainly by reduced evaporation.

**Keywords**: Climate change, Craig-Gordon model, deuterium, hydrogen, Keeling plot, mass balance, spectroscopy, stable isotope

# 1. INTRODUCTION

Evapotranspiration (*ET*) plays a critical role in the hydrological cycle and represents the process that links both the energy and water cycles (Wang and Dickinson, 2012). In semi-arid environments, *ET* is a major pathway of water loss and can account for up to 95% of the precipitation input (Huxman et al., 2005; Wang et al., 2012a). Transpiration (*T*), the water vapor loss from plants, is a vegetation-controlled process and *T/ET* ratios reflect the influence of vegetation on the hydrological cycle. *T/ET* changes in response to temperature increases provide important insights into biological feedbacks, especially for those that might occur under potential global warming scenarios. Global warming is expected to increase *ET* and lead to greater aridity in water-limited systems, according to many global climate model simulations (Gleick, 1989; Zavaleta et al., 2003). However, these model predictions usually do not consider biological feedbacks, which may be important in regulating the overall climate change impacts on water cycling. In a recent investigation, it was observed that increased $CO_2$ can improve plant water use efficiency during photosynthesis, possibly counteracting the expected drying due to higher temperatures (Morgan et al., 2011). Nevertheless, the global warming effect on ecosystem *T/ET* changes has not been well investigated and experimental evidence for a warming effect on ecosystem *T/ET* is lacking. Understanding the implications and outcomes of these potential changes in vegetation response to climate change is of considerable importance.

Water isotopes are useful tracers in ecosystem hydrology (Dawson et al., 2002). The stable isotope composition ($\delta^2$H, $\delta^{18}$O) is defined as $\delta = (R/R_{std} - 1)$, where $R$ is the ratio of rare to common isotope ($^2$H/$^1$H or $^{18}$O/$^{16}$O) of a sample, and $R_{std}$ is the ratio of the

international standard on the *V-SMOW* (Vienna Standard Mean Ocean Water)-*SLAP* (Standard Light Antarctic Precipitation) scale. These isotopes can, for example, help identify plant water sources (Dawson and Ehleringer, 1991), hydraulic redistribution (Dawson, 1993), groundwater recharge rates (Cane and Clark, 1999) as well as differential rooting depth among adjacent plants (Jackson et al., 1999). Most applications have used liquid water extracted from soils and plants to follow these ecosystem processes, but recent advances in laser spectroscopy have allowed for water vapor isotopes to be measured *in situ* at high temporal resolution (e.g., 1 Hz) with analytical uncertainties similar to traditional cryogenic trapping methods (Wen et al., 2008; Wang et al., 2009; Wang et al., 2010; Griffis et al., 2011; Zhao et al., 2011). The development of such systems allows for the direct use of $\delta^2$H and $\delta^{18}$O to study water vapor dynamics, including the partitioning of *ET* into *T* and evaporation (*E*) (Wang et al., 2010). These new approaches extend previous work that relied on cryogenic trapping (Harwood et al., 1998; Moreira et al., 2003; Newman et al., 2010).

Both $\delta^2$H and $\delta^{18}$O provide a unique tool for *ET* partitioning (e.g., calculating *T/ET* ratios). The basis for using $\delta^2$H and $\delta^{18}$O to partition *ET* is that evaporation significantly fractionates the surface soil water (Luz et al., 2009). Plants, however, do not fractionate water during uptake (White et al., 1985; Ehleringer and Dawson, 1992). The isotopic composition of transpiration ($\delta_T$) is therefore assumed to be equal to the isotopic composition of plant source water. This assumption is generally valid for timescales much greater than the turnover time of water in the leaves and in the absence of rapidly changing environmental conditions because mass balance constraints require that the $\delta_T$ should be equal to that of the soil water in the rooting zone. This results in

distinct isotopic compositions of evaporation ($\delta_E$) and $\delta_T$. By measuring the isotopic end members ($\delta_E$ and $\delta_T$) along with the isotopic composition of aggregated *ET* ($\delta_{ET}$), the *T/ET* ratios can be calculated via mass balance (Wang et al., 2012a). $\delta_{ET}$ is typically measured using a Keeling plot approach in which isotopic compositions of water vapor are measured at several heights above the canopy (Keeling, 1958). The resulting gradient in water vapor concentration and isotopic composition is used to extrapolate $\delta_{ET}$ derived from the ecosystem. The $\delta_T$ is typically measured using xylem or stem water under the assumption that the isotopic composition of xylem water is equivalent to $\delta_T$ under isotopic steady state (e.g., Yepez et al., 2005). The assumption of isotopic steady state can be made during times of high transpiration rate and stable vapor pressure deficit (Harwood et al., 1998): but the diurnal periods during which this applies depend on environmental conditions and plant species. Wang et al. (2012b) developed and verified a new method that uses a mass balance approach to calculate $\delta_T$ from *in situ* chamber measurements, which is applicable for both steady state and non-steady state conditions and is applicable to estimate $\delta_{ET}$ and $\delta_E$. The $\delta_E$ has commonly been estimated using the Craig-Gordon evaporative fractionation model (Craig and Gordon, 1965), although numerical isotope modeling efforts are also widely used (Mathieu and Bariac, 1996; Braud et al., 2009; Haverd et al., 2011; Soderberg et al., in press).

The $\delta^2$H and $\delta^{18}$O values between plant organic matter and liquid water in both leaf and surrounding environments provide important information on current and past environments (Terwilliger et al., 2002; McCarroll and Loader, 2004; Helliker, 2011). The utility of these liquid-organic isotopic relationships for generating information about the entire Soil-Plant-Atmosphere-Continuum (*SPAC*) depends on an understanding of

how water isotopes change throughout the *SPAC*, including under warming conditions. Here we present work that demonstrates the effectiveness of coupled laser spectroscopy-chamber based isotope techniques for measuring *ET* partitioning. The work was performed under ambient and artificially warmed conditions to evaluate the effects of warming on the sources of contributions to *ET*. The objectives of this study are to: 1) evaluate the performance of multiple isotope-based *ET* partition methods for the estimation of $\delta_E$, $\delta_{ET}$ and $\delta_T$; 2) combine estimates of $\delta_E$, $\delta_{ET}$ and $\delta_T$ to partition *ET*; and 3) assess how warming scenarios influence surface vapor flux partitioning.

## 2. MATERIALS AND METHODS

### 2.1 Study site

The study was conducted at the University of Oklahoma's Kessler Farm field laboratory, which is located in central Oklahoma in the Great Plains of the USA (34.982°N, 97.521°W). The mean annual temperature of this site is 16.0°C with monthly mean temperature of 3.1°C in January and 28.0°C in July. The mean annual rainfall is 911.4 mm (Oklahoma Meteorological Survey). The study site is an old field dominated by $C_3$ winter annuals of *Bromus arvensis* L. and *Vicia sativa* L. in the spring, and in summer by the $C_3$ forbs *Solanum carolinense* L. and *Euphorbia dentata* Michx. and the perennial $C_4$ grass *Tridens flavus* (L.) Hitchc. The present study took advantage of the experimental setup of a long-term multiple-factor climate control experiment, which was established in 2009 to quantify main versus interactive effects of experimental warming, added and reduced precipitation, biomass harvesting on ecosystem processes and community structure. We utilized only the warming and control plots without biomass

harvesting and precipitation treatments. Warming is maintained using infrared heaters and the air temperature is approximately 2°C above the ambient. One ‘‘dummy’’ heater, made of metal flashing with the same size and shape as the infrared heaters, was suspended in each control plot at the same height and position as in the warmed plots to exclude the potential effect of shading. Four warming plots and four control plots were used. Five extensive field samplings were conducted on May 31, June 3, June 5, June 7 and June 8, 2011 (only two warming and two control plots were measured on June 3 due to pump failure). There were seven rainfall events in May (1, 8, 11, 12, 19, 20 and 24) with a total rainfall of 88 mm for the month preceding the measurements. No rainfall events occurred during the measurement period. The vegetation and litter cover survey was conducted using a grid method on June 8 for all the measured plots. A 1 m x 0.5 m double grid frame defining 50 points was placed in each plot. For each of the 50 points, the presences of either a $C_3$ plant, a $C_4$ plant, litter or bare ground was recorded. Percent plant or litter cover was calculated as the number of total hits of plant or litter from the grid frame data divided by the total number of hits (50) and multiplied by 100. On June 5$^{th}$ the amount of $E$ and $ET$ (mmol m$^{-2}$ s$^{-1}$) were measured using Licor instruments (Licor 6400 and Licor 8100, LI-COR Biosciences, Lincoln, NE, USA) on permanently installed collar and metal frame at each plot.

**2.2 Isotopic flux partitioning**

The fraction of $ET$ derived from transpiration is found through measurement of two isotopic end members ($\delta_E$ and $\delta_T$) and $\delta_{ET}$. Given a simple two-part mixing model the transpired fraction is given by

$$\frac{T}{ET} = \frac{\delta_{ET} - \delta_E}{\delta_T - \delta_E}$$ (e.g., Wang et al., 2010). (1)

The isotopic compositions of vapor fluxes ($\delta_E$, $\delta_{ET}$ and $\delta_T$) were directly quantified from each plot using a commercially available and field deployable water vapor isotope analyzer (WVIA, DLT-100, Los Gatos Research, Mountain View, CA, USA) in conjunction with various chambers.

Multiple methods have been used to estimate the isotopic composition of vapor fluxes, including the Keeling plot approach, mass balance approach, the Craig-Gordon model and assumptions based on soil extracted water isotopic values (Wang et al., 2012b; Good et al., 2012). The Keeling plot approach assumes constant concentrations and isotopic compositions of the background water vapor. The isotopic compositions of source water vapor (e.g., evaporation, transpiration or evapotranspiration) can be calculated as:

$$\delta^2 H_M = c_A(\delta^2 H_A - \delta^2 H_s)(1/c_M) + \delta^2 H_S \quad , \tag{2}$$

where $\delta^2 H_M$, $\delta^2 H_A$ and $\delta^2 H_S$ are the isotopic compositions of mixed water vapor, ambient water vapor and source water vapor respectively, $c_M$ is the mixed water vapor concentration, and $c_A$ is the ambient water vapor concentration at the measurement location. The temporal Keeling plot approach (e.g., $\delta^2 H_M$ varies with time due to source additions) was used for $\delta_E$, $\delta_{ET}$ and $\delta_T$ estimates. A recent report on the techniques suitability for assessing the isotopic composition of fluxes found time-based Keeling plots are of similar precision to those based on measurements of vertical profiles, given that variability in vapor concentrations are similar (Good et al., 2012).

The calculation of source water vapor isotopic composition using a mass balance approach is calculated as:

$$\delta^2 H_s = \frac{C_M \delta_M - C_A \delta_A}{C_M - C_A} \quad , \tag{3}$$

where $\delta^2H_s$ is the isotopic composition of source water vapor (e.g., plant transpired water or evaporation), $C_A$ and $C_M$ are the concentrations of ambient and mixed water vapor in the chamber [mol $m^{-3}$], and $\delta_A$ and $\delta_M$ are the isotopic compositions of ambient and mixed water vapor in the chamber. The mass balance approach has been applied to directly quantify $\delta_T$ using the laser-based analyzer and transparent leaf chamber (Wang et al., 2012b). A similar setup and calculation procedure was used for $\delta_E$, $\delta_{ET}$ and $\delta_T$ estimates.

The Craig-Gordon model is a traditional way to estimate $\delta_E$, and is calculated as:

$$\delta_E = \frac{\alpha\delta_L - \delta_A h - \varepsilon_K - \varepsilon^*}{(1-h) + 10^{-3}\varepsilon_K}, \quad (4)$$

where $\delta_E$ is the isotopic composition of water evaporated from the soil, $\alpha$ is the temperature-dependent equilibrium fractionation factor (formulated here as the ratio of the vapor phase to liquid phase isotope ratios), which can be calculated based on soil temperature (Majoube, 1971), $\delta_L$ is the isotopic composition of liquid water at the evaporating front, $\delta_A$ is the isotopic composition of the ambient atmospheric water vapor, $\varepsilon^*$ is calculated as (1-$\alpha$), $\varepsilon_K$ is the kinetic fractionation factor for hydrogen, and $h$ is the relative humidity normalized to the surface soil temperature (Craig and Gordon, 1965; Horita et al., 2008). The $\varepsilon_K$ is calculated as

$$\varepsilon_K = n(1-h)\left(\frac{D}{D_i} - 1\right)\frac{r_m}{r} \times 10^3, \quad (5)$$

where $h$ is the relative humidity normalized to the surface soil temperature, $D$ and $D_i$ are the diffusivities of the light and heavy isotopologue, with the ratio 1.0251 for hydrogen (Merlivat, 1978). The "weighting term" $r_m/r$ is assumed to be 1 for small water bodies. The aerodynamic parameter $n$ is taken as 0.5 for turbulent conditions between the

evaporating surface and the free atmosphere, and 1.0 for completely laminar flow as in dry soils. This parameter can be adjusted from 0.5 in wet soils to 1.0 in dry soils (Mathieu and Bariac, 1996). We set *n* to 1.0 for our soil moisture levels (1-3 % by volume), which are relatively dry, and likely close enough to "residual" moisture content for *n* to be very close to 1.0 (e.g., Soderberg et al., in press).

**2.3 Isotopic composition of vapor fluxes**

Three methods were used for $\delta_T$ calculation: 1) temporal Keeling plot approach (equation 2); 2) the mass balance method (equation 3) (Wang et al., 2012b); and 3) the measured isotopic composition of soil extracted water, assuming $\delta_T$ is equal to the isotopic composition of source water. For both the Keeling plot and mass balance method, the $\delta_M$ value was measured using the WVIA with a transparent leaf chamber modified from a LI-COR conifer chamber (part No. 6400-05, LI-COR Biosciences, Lincoln, NE, USA). The specifics of the leaf chamber have been reported elsewhere (Wang et al., 2012b). To summarize the configuration, the leaf chamber is made of Teflon lined transparent plastic with a volume of 150 $cm^3$. The chamber has a residence time of 18 seconds at a flow rate of 500 $cm^3$ per minute. The base plate of the chamber was removed and a 1/4" brass bulkhead was installed to allow the WVIA inlet to connect to the chamber base.

Three methods were used for $\delta_E$ calculation: 1) the Craig-Gordon model using soil extracted water isotopic composition and measured environmental factors; 2) the mass balance method (Wang et al., 2012b); and 3) the temporal Keeling plot approach (equation 2). For the Craig-Gordon model, the $\delta_A$ was measured using the WVIA, the temperature and relative humility values were obtained using direct iButton

measurements (model No. DS1923-F5#, Maxim, Sunnyvale, CA, USA) at the soil surface of each plot. For the Keeling plot and mass balance calculations, the $\delta_M$ value was measured using the WVIA and a LI-COR soil chamber (part No. 6400-09, LI-COR Biosciences, Lincoln, NE, USA), which was placed on a permanently installed PVC collar at each plot. One soil sample (0-2 cm depth) was collected along with each $\delta_E$ measurement for soil water extraction.

Two methods were used for $\delta_{ET}$ calculation: the temporal Keeling plot approach (equation 2); and the mass balance method (equation 3) (Wang et al., 2012b). The $\delta_{ET}$ value was determined using the WVIA and a customized transparent chamber with a dimension of 50 x 50 x 50 cm placed on a permanently installed metal frame at each plot. The field measurements were conducted typically between 7:30 am to 2:00 pm. The WVIA was covered by thick cloth during the operations to minimize direct radiative heating. The $\delta_E$, $\delta_{ET}$ and $\delta_T$ measurements were sampled randomly for each plot. Due to instrumental malfunctions and obvious data errors (e.g., $\delta_E > \delta_T$), some of the chamber-based data were excluded from analyses. Overall, 92% of $\delta_{ET}$, 89% of $\delta_T$ and 69% $\delta_E$ data were usable when combining mass balance and Keeling plot approaches. If the data from the first sampling date were excluded, the successful rates were much higher (e.g., 100% for $\delta_{ET}$, 96% for $\delta_T$ and 82% for $\delta_E$).

**2.4 Laboratory analyses of soil liquid isotopic composition**

The collected soil samples were kept cool while in the field and sieved through 2 mm mesh, with fine roots and plant debris being removed in the laboratory. The soil samples were then frozen for later analysis. The soil samples were extracted at Princeton University using a traditional glass-line system similar to that of West et al. (2006). The

soil water extracts were measured using the WVIA coupled with a water vapor isotope standard source (Los Gatos Research, Mountain View, CA, USA), which completely vaporizes a droplet (<1 $\mu$L) of water without inducing fractionation. The $\delta^2$H precision of the WVIA measurements is 1.0 ‰ when 1 Hz data are aggregated over 1-3 minutes (Wang et al., 2009).

### 2.5 Statistical analyses

To test the warming effect on end member estimates and on *ET* partitioning, two-way ANOVA with sampling date and treatment (warming vs. control) as two main factors was used and a Tukey *post hoc* test was employed to separate the means when significant effects were found for any main factors.

## 3. RESULTS

### 3.1 Method comparisons for $\delta_E$, $\delta_{ET}$ and $\delta_T$ estimates

To evaluate the performance of each method for estimating of $\delta_E$, $\delta_{ET}$ and $\delta_T$, estimates of isotopic composition from the different methods were compared against each other. The chamber-based mass balance approach and the Keeling plot approach compared favorably with each other for $\delta_{ET}$ estimates, with a slope of 0.82 and $R^2$ of 0.89 (Fig. 1). The chamber-based mass balance approach and Keeling plot approach also showed good agreement for $\delta_T$ (Fig. 2) and $\delta_E$ (Fig. 3) estimates, with a slope of 0.92 and 1.04, and $R^2$ of 0.81 and 0.86 respectively, for $\delta_T$ and $\delta_E$. The chamber-based $\delta_T$ estimates were generally lighter than the soil extracted water isotopic compositions (-66.9 ± 15.3‰ vs. -48.0 ± 9.9‰ for chamber-based $\delta_T$ and soil water isotopic compositions, respectively) indicating that vegetation utilizes soil water deeper than 2 cm (the soil

sampling depth) in this ecosystem and that the deeper soils are less subject to surface evaporation enrichment. These results indicate that using isotopic compositions of soil water extraction to represent $\delta_T$ may be subject to errors in this system and therefore only the chamber-based method results were used in partitioning *ET* in this study. Though the mass balance and Keeling plot $\delta_E$ values agreed well with each other (Fig. 3), neither method agreed with the Craig-Gordon model based values (Fig. 4). The $\delta_E$ values of both chamber-based methods were consistently more enriched than the Craig-Gordon model calculations (Fig. 4). The enrichment was 12‰ on average.

**3.2 Warming effects on water isotopic compositions**

The sampling dates did not have any significant effect on the isotopic compositions across all three fluxes ($p > 0.05$). The warming significantly decreased both the isotopic compositions of soil liquid water and $\delta_E$, calculated by the Craig-Gordon model using soil liquid water isotopic compositions and measured environmental parameters (Fig. 5). The isotopic compositions of soil water were -43.3 ± 10.0‰ and -54.0 ± 6.2‰ ($p < 0.05$) respectively, for control and warming treatments. The $\delta_E$ were -134.3 ± 20.9‰ and -167.3 ± 44.5‰ ($p < 0.05$) respectively, for control and warming treatments. Warming did not significantly affect $\delta_T$ and $\delta_{ET}$ ($p > 0.05$). The $\delta_T$ of the control and warming treatments were -63.5 ± 16.1‰ and -69.7 ± 14.5‰ respectively. The $\delta_{ET}$ of the control and warming treatments were -80.3 ± 14.0‰ and -82.5 ± 12.6‰ respectively.

**3.3 Warming effects on *ET* partition**

Based on the direct measurements on June 5, 2011, the warming did not affect total *ET,* but did decrease *E* (Fig. 6). The *ET* was 1.82 ± 0.60 and 1.07 ± 0.92 mmol $m^{-2}$

$s^{-1}$ ($p > 0.05$) for control and warming treatments respectively. The $E$ was 0.13 ± 0.08 and 0.04 ± 0.01 mmol $m^{-2}$ $s^{-1}$ ($p = 0.061$) respectively, for control and warming treatments (Fig. 6). These direct measurements are only available for a single day due to time and sampling constraints. Further analyses of the warming effects are assessed through isotope flux partitioning.

Because of the discrepancies between the Craig-Gordon model and chamber-based estimates of $\delta_E$, two methods were used to calculate the *ET* partitioning. Both methods used chamber-based estimates of $\delta_{ET}$ and $\delta_T$, but method 1 used the chamber-based $\delta_E$ (Craig-Gordon model based numbers were used for missing values) and method 2 used the Craig-Gordon model based $\delta_E$ estimates, to calculate *T/ET* ratios under the control and warming treatments. Both methods showed a significant increase in *T/ET* ratios under the warming treatments (Fig. 7). Method 1 resulted in 0.65 ± 0.21 and 0.83 ± 0.12 ($p < 0.05$) in *T/ET* ratios under the control and warming treatments respectively; and method 2 resulted in 0.77 ± 0.15 and 0.86 ± 0.10 ($p < 0.05$) in *T/ET* ratios under the control and warming treatments respectively (Fig. 7). There was a positive relationship between vegetation cover and *T/ET* ratios (the relationship is similar using method 2 results and method 1 results), and vegetation cover explained 37% of the total variance in *T/ET* ratios (Fig. 8).

## 4. DISCUSSION

### 4.1 Method comparisons for $\delta_E$, $\delta_{ET}$ and $\delta_T$ estimates

The Keeling plot approach has been widely used to calculate the isotopic compositions of source $CO_2$ (Keeling, 1958; Pataki et al., 2003). Recently the same principle has been used to calculate the $\delta_{ET}$ at both chamber (Yepez et al., 2005) and

ecosystem scales (Moreira et al., 2003) using the traditional cold-trap method. Wang et al. (2010) extended the Keeling plot $\delta_{ET}$ estimate to direct measurements using a laser-based instrument. Theoretically the Keeling plot principle can also be used for estimates of $\delta_E$ and $\delta_T$, but such reports are not readily seen in the literature. Wang et al. (2012b) developed and verified a new method based on the mass balance of both water vapor and isotopes inside the leaf chamber to calculate $\delta_T$. The method is applicable for both steady state and non-steady state conditions and is also able to estimate $\delta_{ET}$ and $\delta_E$. If we rearrange the Keeling plot calculation (equation 2) to solve $\delta^2 H_S$, we can form the same solution as expressed in equation 3. That is, mathematically the Keeling plot approach is identical to the steady-state solution of the mass balance approach. In the current study, the chamber-based mass balance approach and the Keeling plot approach did compare favorably with each other for $\delta_{ET}$, $\delta_T$ and $\delta_E$ estimates (Figs. 1-3). The discrepancies are caused by different time periods used for the two methods: the Keeling plot approach used measurements from the "chamber on" periods only and the mass balance approach used measurements from both ambient periods and "chamber on" periods. It is difficult to evaluate which method is more accurate without a third independent technique for comparison. However, the mass balance approach explicitly considers the isotopic compositions of ambient air, whereas the Keeling plot approach avoids using measured ambient values in calculations. The Keeling plot approach is likely advantageous for capturing the initial rapid changes before reaching steady state, but less powerful under steady state condition when observed values become constant.

The $\delta_E$ is commonly calculated using the Craig-Gordon model. In the current study, though the mass balance and Keeling plot $\delta_E$ values agreed well with each other

(Fig. 3), neither agreed with the Craig-Gordon model based values (Fig. 4). The $\delta_E$ values of both chamber-based methods were consistently more depleted than the Craig-Gordon model calculations (Fig. 4). A recent study showed that the Craig-Gordon model could be improved by considering the soil water potential in dry soils (Soderberg et al., in press). Unfortunately, soil water potentials were not measured from this experiment and such discrepancies require further investigation. Considering the inconsistency with the Craig-Gordon model results and relatively lower successful measuring rates (~70%), the employment of chamber-based $\delta_E$ measurements need to be more cautious especially for lower evaporation flux conditions. Nevertheless, this study demonstrates for the first time, that it is feasible to use coupled chamber-laser based instrument methods to quantify the isotopic compositions of two end members and $\delta_{ET}$. Because of the capability of field deployment and *in situ* measurements, the coupled chamber-laser instrument method will provide a new opportunity to quantify *ET* partitioning under diverse environmental conditions. The other potential advantage of using the coupled chamber-laser instrument method is the relatively consistent error sources in the isotopic compositions of three fluxes (e.g., from the same laser instrument), which might be diminished or even canceled out when calculating the *ET* partitioning.

**4.2 Warming effects on water isotopic compositions**

Warming significantly decreased both the isotopic compositions of soil liquid water (Fig. 5A) and $\delta_E$ (Fig. 5B) (e.g., the isotopic values were more negative under the warming treatments). Because evaporation tends to enrich the near-surface soil water isotopic compositions (Barnes and Allison, 1988), lower isotopic compositions of both soil liquid water and the evaporated vapor indicate lower evaporation rates under the

warming treatment, which was supported by the direct evaporation measurements (Fig. 6). We suspect the reduced evaporation is due to the shading effect (e.g., reduced radiation) from higher vegetation cover under the warming treatment. The vegetation cover survey during the measurement period did reveal a higher cover under the warming treatment (11.6 ± 5.9% vs. 15.2 ± 7.3% for fractional cover of the control and warming respectively). However, these results were not statistically significant, possibly due to high variation within treatments and the small sample size (n = 4). Warming did not significantly affect $\delta_T$ and the consistency in $\delta_T$ between the control and warming treatment indicate that the vegetation water source (e.g., uptake from the same soil layer) did not change under the warming treatments.

**4.3 Warming effects on *ET* partition**

Both methods for *T/ET* calculation showed a significant increase in *T/ET* ratios under the warming treatments (Fig. 7). Values of $\delta_{ET}$ and $\delta_T$ did not change under the warming treatments, and therefore the observed increase in *T/ET* ratio under warming is due mainly to smaller evaporation of water with a more depleted $\delta_E$. Because no consistent patterns in relative humidity and isotopic compositions of ambient air were observed between the control and warming treatments (data not shown), two potential components responsible for $\delta_E$ changes are temperature-dependent equilibrium fractionation factor (α in equation 4) and soil water isotopic composition according to Craig-Gordon model formulation (equation 4). To test the effects of changes in α and soil water isotopic composition on $\delta_E$ and the consequent *T/ET*, Craig-Gordon model calculations were conducted under two scenarios. For the first scenario, the change in $\delta_E$ was calculated with soil temperatures ranging from the average observed observation to

2°C warmer. The temperature change only affects the $\alpha$ values assuming surface temperature is equivalent to air temperature. In this case the observed mean values of relative humidity, air temperature, as well as the isotopic compositions of soil water and ambient air were used and kept constant. Under this scenario, the $\delta_E$ actually increased as temperature increased (Fig. 9A), resulting in slightly decreased *T/ET* ratio (Fig. 9B), which is contrary to the observed trend (Fig. 7). For the second scenario, the $\delta_E$ change was calculated for a range of soil water isotopic compositions. The $\delta_L$ value was forced to decrease as temperature increased, following the observations, and other variables were kept constant at the average observed values. Under this scenario, the $\delta_E$ decreased as temperature increased (Fig. 9C), resulting in increased *T/ET* ratio (Fig. 9D) and matched the observations (Fig. 7). These results indicate that warming-induced decrease in soil water isotopic composition is the major factor responsible for the observed *T/ET* ratio increase. Changes in α due to higher soil temperatures play an insignificant role.

Transpiration response is another important component for *T/ET* trend under warming. At the leaf level, when temperature increases, vapor pressure deficits of the air will increase and result in a concomitant increase in the transpiration rate (Kirschbaum, 2004). However, if there is a reduction in the diurnal temperature range, transpiration rates may decrease (Kirschbaum, 2004). At the ecosystem level, earlier experimental work has showed that warming could reduce transpiration water losses resulting from earlier senescence in an annual-dominated grassland ecosystem (Zavaleta et al., 2003). Based on the current data, we cannot conclusively determine whether vegetation transpiration rates increased or decreased under the warming treatment. We can use the measured *ET* and *E* data to estimate *T* (Fig. 6), which showed similar *T* values between

the control and warming treatments (data not shown). However, unlike the isotope-based partition method where all fluxes are measured using the same instrument, calculated by the same principle, and subject to similar errors, *ET* and *E* are measured independently. Because of the short duration of the measurements and large variation among plots, the calculated *T* under this particular situation may not be conclusive. Based on the observed *E* and $\delta_E$ values, it is very likely that the observed *T/ET* increasing trend under warming is due to reduced soil evaporation, which is caused by increased vegetation cover.

We note that the increases in *T/ET* under the warming treatments were influenced by several prior rainfall events providing adequate soil moisture for vegetation growth. Soil moisture limitation could counteract the increase in *T/ET* or even induce the opposite trends (Jung et al., 2010). Also the results are from a relatively short peak growing period and long-term effects still need to be investigated.

There was a positive relationship between vegetation cover and *T/ET* ratios, with vegetation cover explaining 37% of the total variance in *T/ET* ratios (Fig. 8). The positive relationship between vegetation cover and *T/ET* ratios has been reported in an earlier manipulation experiment conducted inside Biosphere 2 in Arizona, USA (Wang et al., 2010). In that study, the *T/ET* ratio rose from 61% to 83% as woody vegetation cover increased from 25% to 100% (Wang et al., 2010). In the current field-based study, the *T/ET* ratio reached 70%, even with a low vegetation cover of 5%. One potential reason of the high *T/ET* ratio at low vegetation cover is the high litter cover in the experimental plots. The litter covers in the control and warming plots were 38.3 ± 4.6% and 31.8 ± 4.9% respectively, which is likely to reduce evaporation loss.

## 5. CONCLUSIONS

The research described here utilized a long-term grassland warming site in Oklahoma to test and compare multiple methods to estimate $\delta_T$, $\delta_{ET}$ and $\delta_E$ *in situ* and examine the effect of warming on *ET* partitioning. The $\delta_T$, $\delta_{ET}$ and $\delta_E$ were quantified using a Keeling plot approach and mass balance method, coupling a laser-based isotope analyzer and various chambers. Besides the chamber method, $\delta_E$ was also estimated with the Craig-Gordon model based on distilled soil water and measured environmental parameters.

Here we show for the first time that it is feasible to use coupled chamber-laser instrument method to quantify the isotopic compositions of all three end members. The chamber method works well for $\delta_T$ and $\delta_{ET}$ estimates, based on agreement between the Keeling plot and mass balance approaches. The chamber method may not always be successful for estimating $\delta_E$, especially when evaporation is very low. Because of the capability of field deployment and *in situ* measurements, the coupled chamber-laser instrument method can provide an improved capacity to quantify *ET* partitioning over a range of scenarios, offering a means of describing this important biophysical response.

The results showed no change in $\delta_T$ and $\delta_{ET}$, but there was a significant decrease in the isotopic composition of soil liquid water and $\delta_E$ under the warming treatment. These changes are likely caused by the higher vegetation cover and lower litter cover under the warming treatment, although neither of these variables was significantly different. The Craig-Gordon model calculations under two scenarios indicate that warming induced decrease in soil water isotopic composition is the major factor responsible for the observed $\delta_E$ trend and warming-induced changes in α play an insignificant role. The results showed an increase in the *T/ET* ratio for the warming

treatments compared to the control treatments. We found the ratio of *T/ET* in the control treatment was about 0.65 or 0.77 and the ratio found in the warming treatment was about 0.83 or 0.86, based on the different methods employed. Based on the observed *ET*, *E* and $\delta_E$ values, we argue that the increased *T/ET* ratio under warming is caused mainly by reduced *E*, with minimal change in *ET* and *T*. We also found a positive relationship between *T/ET* ratio and vegetation cover combining the control and warming treatments. These results suggest a positive feedback of biological effects on hydrological cycles under warming scenarios and may provide valuable information for constraining model predictions of future change.

## 6. ACKNOWLEDGMENTS

This activity was funded by an NSF CAREER award to K. Caylor (EAR 847368) as well as DOE NICCR DE-FC02-06ER64158 to Y. Luo. We appreciate the logistical assistance from Lizzie King of University of Georgia and Frances O'Donnell of Princeton University. We appreciate the field assistance from Dr. Dejun Li, Ding Guo and Erin Reese as well as graph assistance from Dr. Jin Wang. Lixin Wang acknowledges the financial support from Vice-Chancellor's postdoctoral research fellowship of University of New South Wales. We thank two anonymous reviewers and editor Dr. Marc Norman for constructive comments.

## 7. REFERENCES

Barnes C. J. and Allison G. B. (1988) Tracing of water movement in the unsaturated zone using stable isotopes of hydrogen and oxygen *Journal of Hydrology* **100**, 143-176.

Braud I., Bariac T., Biron P. and Vauclin M. (2009) Isotopic composition of bare soil evaporated water vapor. Part II: Modeling of RUBIC IV experimental results. *Journal of Hydrology* **369**, 17-29.
Cane G. and Clark I. D. (1999) Tracing gound water recharge in an agricultural watershed with isotopes. *Ground Water* **37**, 133-139.
Craig H. and Gordon L. I. (1965) Deuterium and oxygen-18 variations in the ocean and marine atmosphere, In *Proceedings of the conference on stable isotopes in oceanographic studies and paleotemperatures* (eds. E Tongiorgi). Laboratory of Geology and Nuclear Science, Pisa, pp. 9–130.
Dawson T. E. (1993) Hydraulic lift and water use by plants: implications for water balance, performance and plant-plant interactions. *Oecologia* **95**, 565-574.
Dawson T. E. and Ehleringer J. R. (1991) Streamside trees that do not use stream water. *Nature* **350**, 335-337.
Dawson T. E., Mambelli S., Plamboeck A. H., Templer P. H. and Tu K. P. (2002) Stable isotope in plant ecology. *Annu. Rev. Ecol. Syst.* **33**, 507-559.
Ehleringer J. and Dawson T. (1992) Water uptake by plants: perspectives from stable isotope composition. *Plant Cell Environment* **15**, 1073–1082.
Gleick P. H. (1989) Climate change, hydrology, and water resources. *Rev. Geophys.* **27**, 329-344.
Good S., Soderberg K., Wang L. and Caylor K. (2012) Uncertainties in the assessment of the isotopic composition of surface fluxes: A direct comparison of techniques using laser-based water vapor isotope analyzers. *Journal of Geophysical Research* **117**, D15301.
Griffis T., Lee X., Bake J., Billmark K., Schultz N., Erickson M., Zhang X., Fassbinder J., Xiao W. and Hu N. (2011) Oxygen isotope composition of evapotranspiration and its relation to C-4 photosynthetic discrimination. *Journal of Geophysical Research-Biogeosciences* **116**, G01035, doi:01010.01029/02010JG001514.
Harwood K., Gillon J. and Griffiths H. (1998) Diurnal variation of $\Delta^{13}CO_2$, $\Delta C^{18}O^{16}O$ and evaporative site enrichment of $\delta H_2{}^{18}O$ in Piper aduncum under field conditions in Trinidad. *Plant Cell Environment* **21**, 269-283.
Haverd V., Cuntz M., Griffith D., Keitel C., Tadros C. and Twining J. (2011) Measured deuterium in water vapour concentration does not improve the constraint on the partitioning of evapotranspiration in a tall forest canopy, as estimated using a soil vegetation atmosphere transfer model. *Agricultural and Forest Meteorology* **151**, 645-654.
Helliker B. R. (2011) On the controls of leaf-water oxygen isotope ratios in the atmospheric Crassulacean Acid Metabolism epiphyte *Tillandsia usneoides*. *Plant Physiology* **155**, 2096-2107.
Horita J., Rozanski K. and Cohen S. (2008) Isotope effects in the evaporation of water: a status report of the Craig-Gordon model *Isotopes in Environmental and Health Studies* **44**, 23 - 49
Huxman T., Wilcox B., Breshears D. D., Scott R. L., Snyder K. A., Small E. E., Hultine K., Pittermann J. and Jackson R. (2005) Ecohydrological implications of woody plant encroachment. *Ecology* **86**, 308-319.

Jackson R., Moore L., Hoffmann W., Pockman W. and Linder C. (1999) Ecosystem rooting depth determined with caves and DNA. *Proceedings of the National Academy of Sciences, USA* **96**, 11387-11392.
Jung M., Reichstein M., Ciais P., Seneviratne S. I., Sheffield J., Goulden M. L., Bonan G., Cescatti A., Chen J., Jeu R. d., Dolman A. J., Eugster W., Gerten D., Gianelle D., Gobron N., Heinke J., Kimball J., Law B. E., Montagnani L., Mu Q., Mueller B., Oleson K., Papale D., Richardson A. D., Roupsard O., Running S., Tomelleri E., Viovy N., Weber U., Williams C., Wood E., Zaehle S. and Zhang K. (2010) Recent decline in the global land evapotranspiration trend due to limited moisture supply. *Nature* **467**, 951-954.
Keeling C. (1958) The concentration and isotopic abundances of atmospheric carbon dioxide in rural areas. *Geochim Cosmochim Acta* **13**, 322-334.
Kirschbaum M. U. F. (2004) Direct and indirect climate change effects on photosynthesis and transpiration. *Plant Biology* **6**, 242-253.
Luz B., Barkan E., Yam R. and Shemesh A. (2009) Fractionation of oxygen and hydrogen isotopes in evaporating water. *Geochimica et Cosmochimica Acta* **73**, 6697-6703.
Majoube M. (1971) Fractionnement en oxygene-18 et en deuterium entre l'eau et sa vapeur. *J. Chim, Phys.* **68**, 1423-1436.
Mathieu R. and Bariac T. (1996) A numerical model for the simulation of stable isotope profiles in drying soils. *Journal of Geophysical Research* **101**, 12685-12696.
McCarroll D. and Loader N. J. (2004) Stable isotopes in tree rings. *Quaternary Science Reviews* **23**, 771-801.
Merlivat L. (1978) Molecular diffusivities of $H_2\ ^{16}O$, $HD^{16}O$, and $H2\ ^{18}O$ in gases *Journal of Chemical Physics* **69**, 2864-2871
Moreira M., Sternberg L., Martinelli L., Victoria R., Barbosa E., Bonates L. and Nepstad D. (2003) Contribution of transpiration to forest ambient vapour based on isotopic measurements. *Global Change Biology* **3**, 439 - 450.
Morgan J. A., LeCain D. R., Pendall E., Blumenthal D. M., Kimball B. A., Carrillo Y., Williams D. G., Heisler-White J., Dijkstra F. A. and West M. (2011) $C_4$ grasses prosper as carbon dioxide eliminates desiccation in warmed semi-arid grassland. *Nature* **476**, 202-205.
Newman B. D., Breshears D. D. and Gard M. O. (2010) Evapotranspiration partitioning in a semiarid woodland: ecohydrologic heterogeneity and connectivity of vegetation patches *Vadose Zone* **9**, 561-572, doi: 510.2136/vzj2009.0035
Pataki D. E., Ehleringer J. R., Flanagan L. B., Yakir D., Bowling D. R., Still C. J., Buchmann N., Kaplan J. O. and Berry J. A. (2003) The application and interpretation of Keeling plots in terrestrial carbon cycle research. *Global Biogeochem. Cycles* **17**, 1022, doi:1010.1029/2001GB001850.
Soderberg K., Good S. P., Wang L. and Caylor K. (in press) Stable isotopes of water vapor in the vadose zone: A review of measurement and modeling techniques. *Vadose Zone Journal* 10.2136/vzj2011.0165.
Terwilliger V. J., Betancourt J. L., Leavitt S. W. and Van de water P. K. (2002) Leaf cellulose δD and $\delta^{18}O$ trends with elevation differ in direction among co-occurring, semiarid plant species. *Geochimica et Cosmochimica Acta* **66**, 3887-3900.

Wang K. and Dickinson R. E. (2012) A review of global terrestrial evapotranspiration: Observation, modeling, climatology, and climatic variability. *Review in Geophysics* **50**, RG2005.
Wang L., Caylor K. and Dragoni D. (2009) On the calibration of continuous, high-precision $\delta^{18}O$ and $\delta^{2}H$ measurements using an off-axis integrated cavity output spectrometer *Rapid Communications in Mass Spectrometry* **23**, 530-536.
Wang L., Caylor K. K., Villegas J. C., Barron-Gafford G. A., Breshears D. D. and Huxman T. E. (2010) Evapotranspiration partitioning with woody plant cover: assessment of a stable isotope technique. *Geophysical Research Letters* **37**, L09401.
Wang L., D'Odorico P., Evans J., Eldridge D., McCabe M., Caylor K. and King E. (2012a) Dryland ecohydrology and climate change: critical issues and technical advances. *Hydrology and Earth System Sciences* **16**, 2585-2603.
Wang L., Good S. P., Caylor K. K. and Cernusak L. (2012b) Direct quantification of leaf transpiration isotopic composition. *Agricultural and Forest Meteorology* **154-155**, 127-135, doi:110.1016/j.agrformet.2011.1010.1018.
Wen X., Sun X., Zhang S., Yu G., Sargent S. and Lee X. (2008) Continuous measurement of water vapor D/H and $^{18}O/^{16}O$ isotope ratios in the atmosphere. *Journal of Hydrology* **349**, 489-500.
West A. G., Patrickson S. J. and Ehleringer J. R. (2006) Water extraction times for plant and soil materials used in stable isotope analysis. *Rapid Communications in Mass Spectrometry* **20**, 1317 - 1321.
White J., Cook E., Lawrence J. and Broecker W. (1985) The D/H ratios of sap in trees: implications for water sources and tree ring D/H ratios. *Geochimica et Cosmochimica* **49**, 237–246.
Yepez E. A., Huxman T. E., Ignace D. D., English N. B., Weltzin J. F., Castellanos A. E. and Williams D. G. (2005) Dynamics of transpiration and evaporation following a moisture pulse in semiarid grassland: A chamber-based isotope method for partitioning flux components. *Agricultural and Forest Meteorology* **132**, 359–376.
Zavaleta E. S., Thomas B. D., Chiariello N. R., Asner G. P., Shaw M. R. and Field C. B. (2003) Plants reverse warming effect on ecosystem water balance. *Proceedings of the National Academy of Sciences* **100**, 9892-9893.
Zhao L., Xiao H., Zhou J., Wang L., Cheng G., Zhou M., Yin L. and McCabe M. F. (2011) Detailed assessment of isotope ratio infrared spectroscopy and isotope ratio mass spectrometry for the stable isotope analysis of plant and soil waters. *Rapid Communications in Mass Spectrometry* **25**, 3071-3082.

**Figure legends**

Figure 1. Comparison of the Keeling plot approach and mass balance approach on chamber-based $\delta_{ET}$ estimates.

Figure 2. Comparison of the Keeling plot approach and mass balance approach on chamber-based $\delta_T$ estimates.

Figure 3. Comparison of the Keeling plot approach and mass balance approach on chamber-based $\delta_E$ estimates.

Figure 4. Comparison of the chamber-based Keeling plot approach, mass balance approach, and Craig-Gordon model based $\delta_E$ estimates.

Figure 5. The effect of warming on soil water isotopic compositions and on $\delta_E$, calculated by the Craig-Gordon model. In the box and whisker plot, the boundary of the box represent $25^{th}$ and $75^{th}$ percentile of the observations, the middle line of the box represent medians of the observations (the dashed lines represent the means), and whiskers above and below the box represent $90^{th}$ and $5^{th}$ percentile of the observations. Different capital letters indicate different means.

Figure 6. The measured evapotranspiration (*ET*) and evaporation (*E*) rates (mmol $m^{-2}$ $s^{-1}$) under the control and warming treatments on June 5, 2011 using Licor instruments. $\alpha$ = 0.1 significance level was used due to small sample size. Refer to the Methods section for measurement details.

Figure 7. The effect of warming on evapotranspiration partition calculated by method 1 (all chamber-based estimates, A) and method 2 (chamber-based estimates for $\delta_{ET}$ and $\delta_T$, Craig-Gordon model based estimates for $\delta_E$, B). In the box and whisker plot, the boundary of the box represent $25^{th}$ and $75^{th}$ percentile of the observations, the middle line of the box represent medians of the observations (the dashed lines represent the means), and whiskers above and below the box represent $90^{th}$ and $5^{th}$ percentile of the observations. Different capital letters indicate different means.

Figure 8. The relationship between vegetation cover and evapotranspiration partition combining the control and warming treatments. The solid line is the linear regression fitted with the least-square method and the dashed lines are 95% confidence interval of the fitted equation.

Figure 9. The effect of changes in temperature dependent equilibrium fractionation factor on $\delta_E$ (A) and consequent *T/ET* ratio (B). Under this condition, only equilibrium fractionation factor varied and other factors (averaged observed values were used) were kept constant. The effect of changes in isotopic composition of soil water ($\delta_{soil}$) on $\delta_E$ (C) and consequent *T/ET* ratio (D). Under this condition, only $\delta_{soil}$ varied and other factors (averaged observed values were used) were kept constant. $\delta_E$ was calculated using Craig-Gordon model. For *T/ET* calculations, $\delta_{ET}$ and $\delta_T$ were the same for the control and

warming treatments. The arrows inside C and D point to the observed isotopic compositions of the soil water under the control and warming treatments.

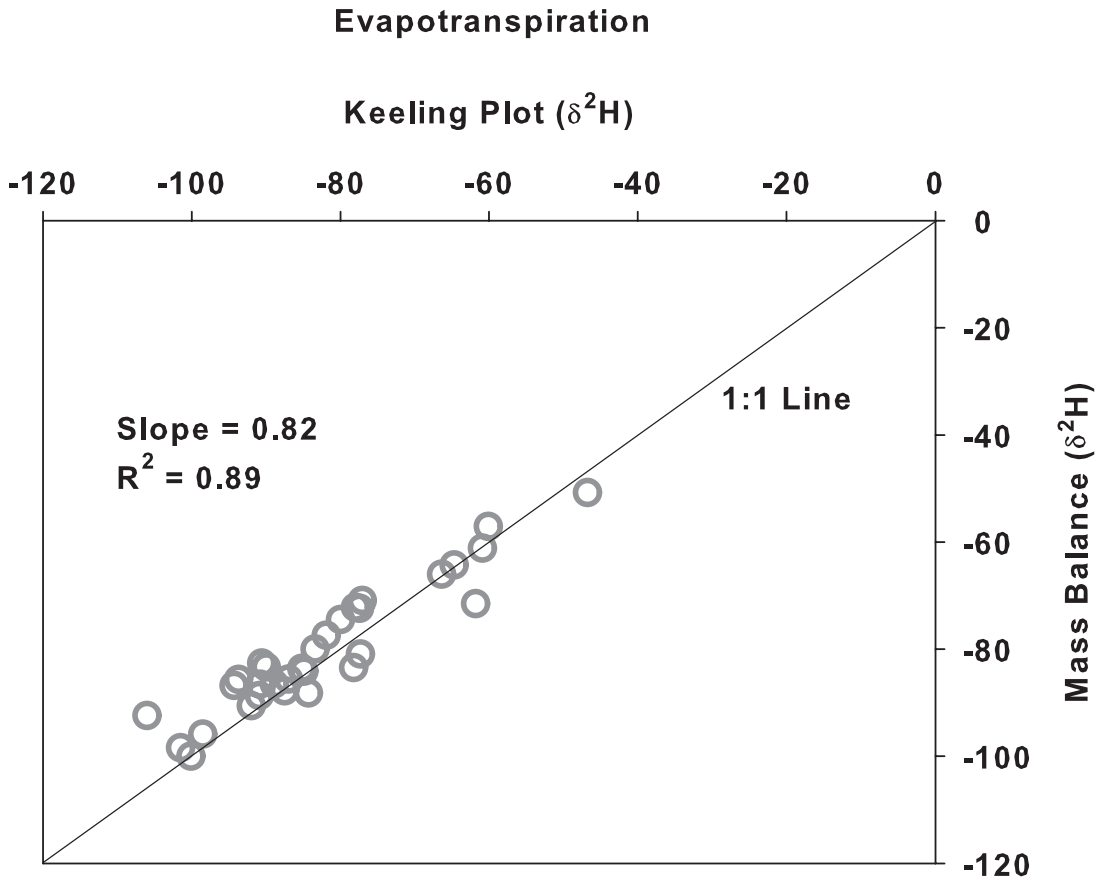
Evapotranspiration
Keeling Plot ($\delta^2H$)
-120
-100
-80
-60
-40
-20
0
0
-20
-40
-60
-80
-100
-120
Mass Balance ($\delta^2H$)
1:1 Line
Slope = 0.82
$R^2$ = 0.89

Figure 1.

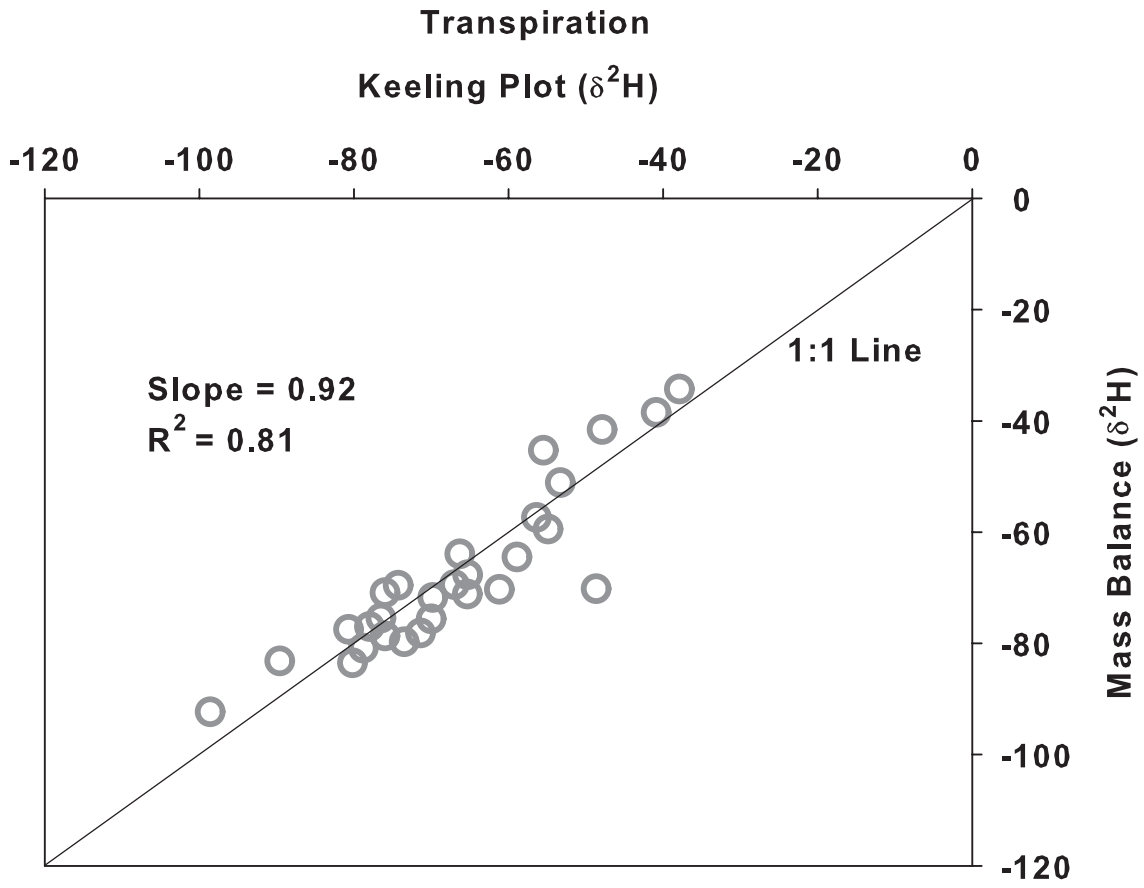
Transpiration
Keeling Plot ($\delta^2H$)
-120
-100
-80
-60
-40
-20
0
0
-20
-40
-60
-80
-100
-120
Mass Balance ($\delta^2H$)
1:1 Line
Slope = 0.92
$R^2$ = 0.81

Figure 2

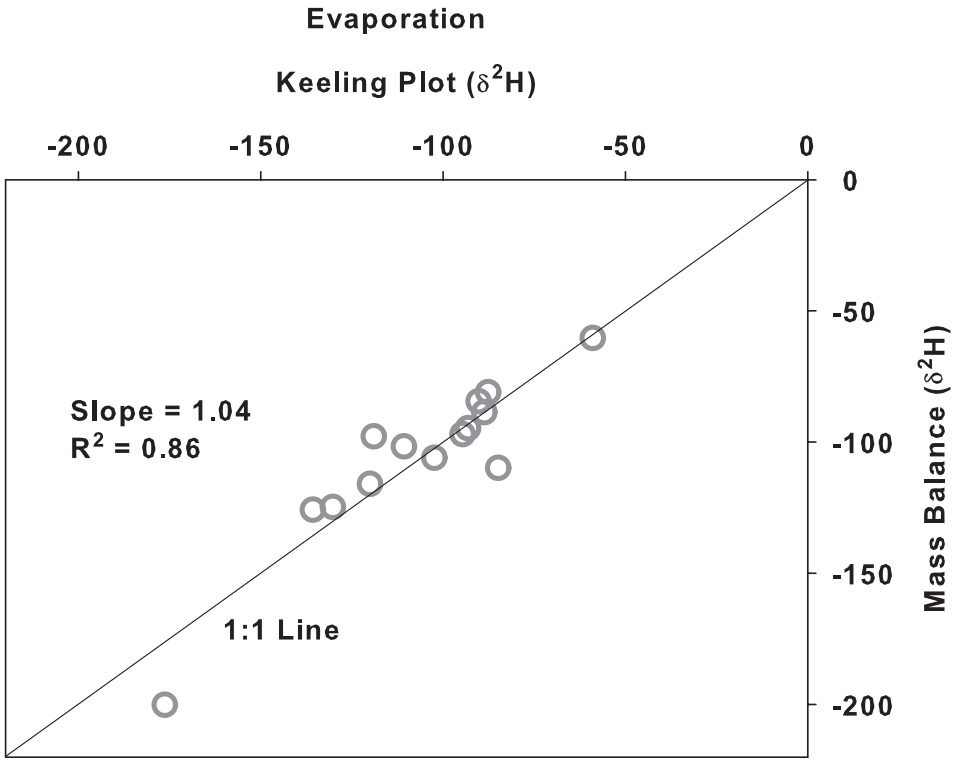
Evaporation
Keeling Plot ($\delta^2H$)
-200
-150
-100
-50
0
0
-50
-100
-150
-200
Mass Balance ($\delta^2H$)
Slope = 1.04
$R^2$ = 0.86
1:1 Line

Figure 3

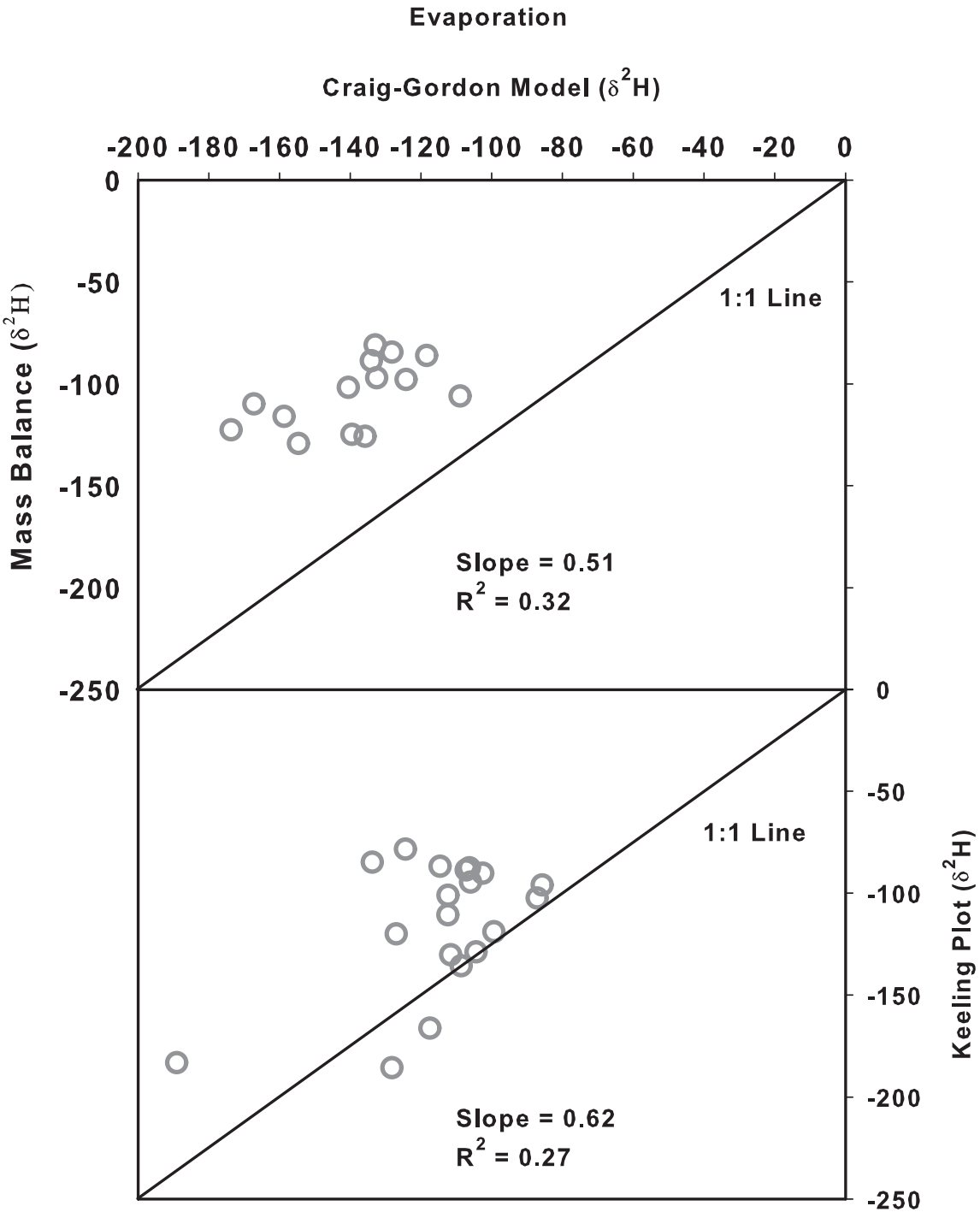
Evaporation
Craig-Gordon Model ($\delta^2$H)
-200 -180 -160 -140 -120 -100 -80 -60 -40 -20 0
0
-50
-100
-150
-200
-250
Mass Balance ($\delta^2$H)
1:1 Line
Slope = 0.51
$R^2$ = 0.32
1:1 Line
Slope = 0.62
$R^2$ = 0.27
0
-50
-100
-150
-200
-250
Keeling Plot ($\delta^2$H)

Figure 4

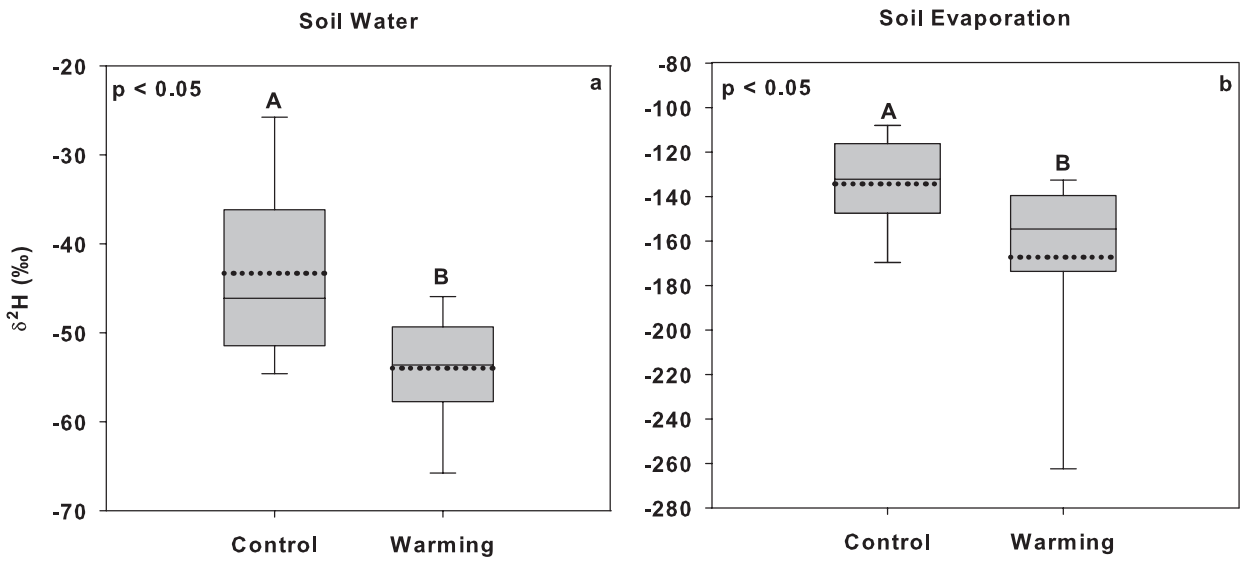
Soil Water
Soil Evaporation
p < 0.05
a
b
A
B
δ²H (‰)
-20
-30
-40
-50
-60
-70
-80
-100
-120
-140
-160
-180
-200
-220
-240
-260
-280
Control
Warming

Figure 5

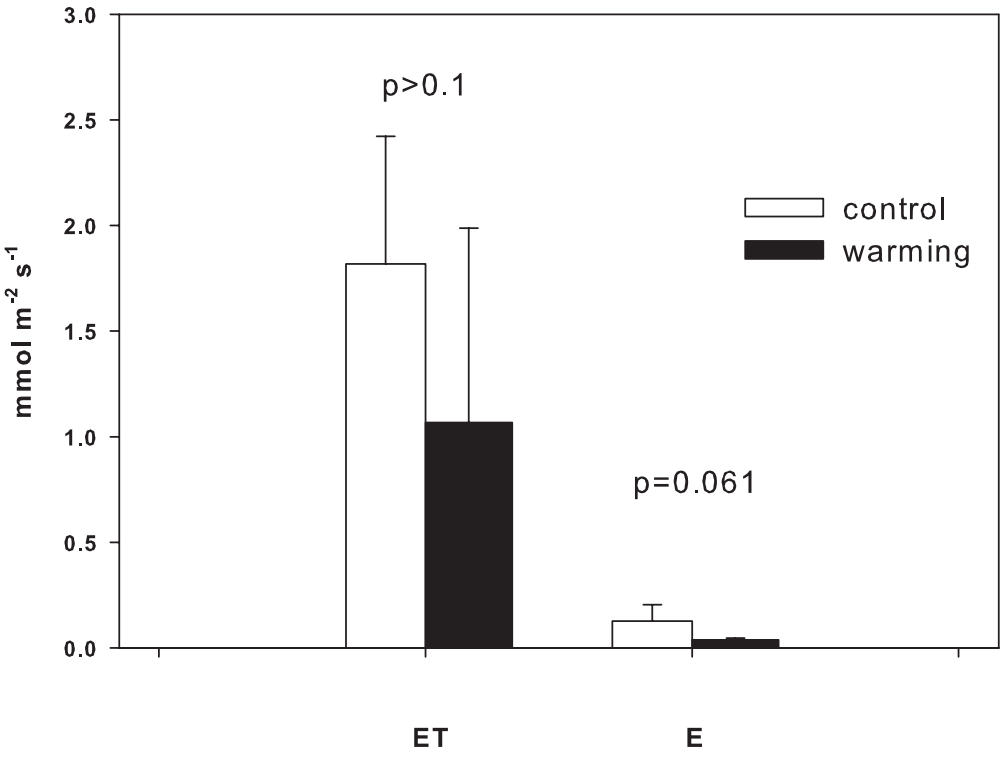


Figure 6

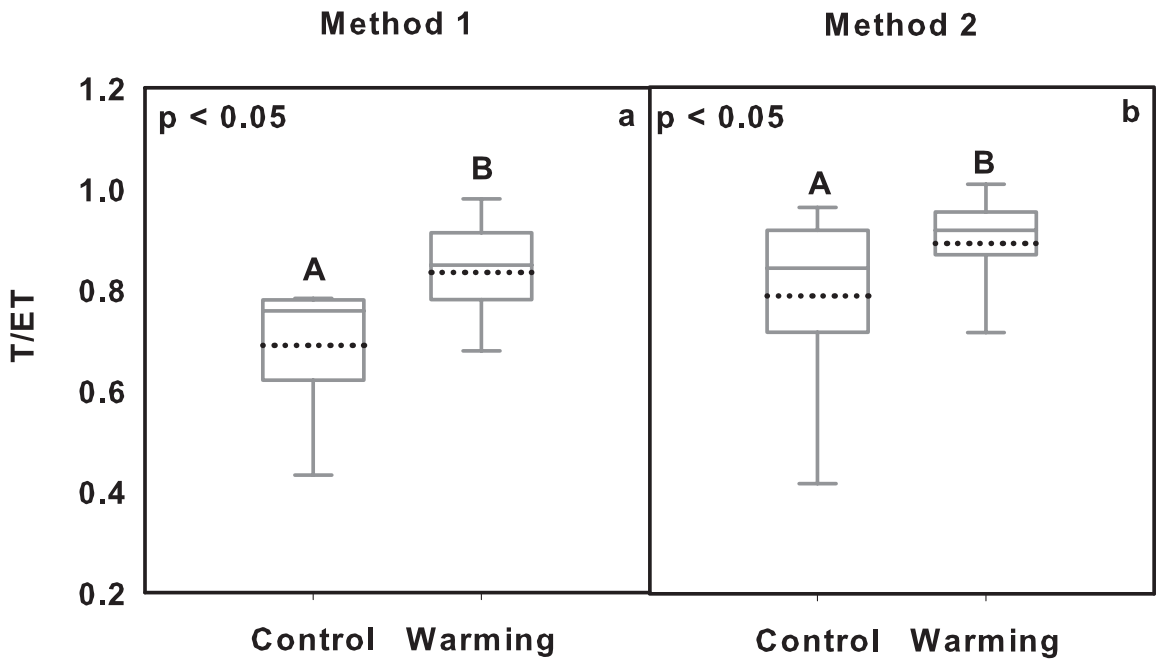
Method 1
Method 2
1.2
1.0
0.8
0.6
0.4
0.2
T/ET
p < 0.05
a
p < 0.05
b
A
B
A
B
Control
Warming
Control
Warming

Figure 7

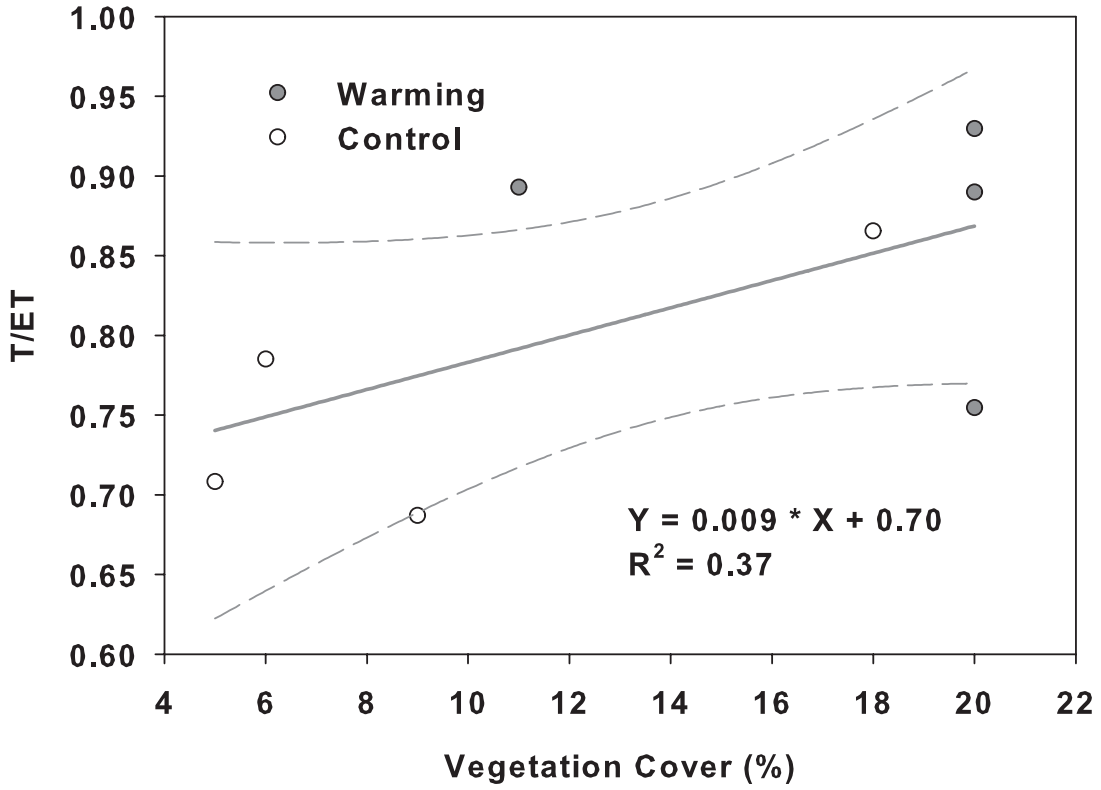
1.00
0.95
0.90
0.85
0.80
0.75
0.70
0.65
0.60
T/ET
Warming
Control
Y = 0.009 * X + 0.70
R2 = 0.37
4
6
8
10
12
14
16
18
20
22
Vegetation Cover (%)

Figure 8

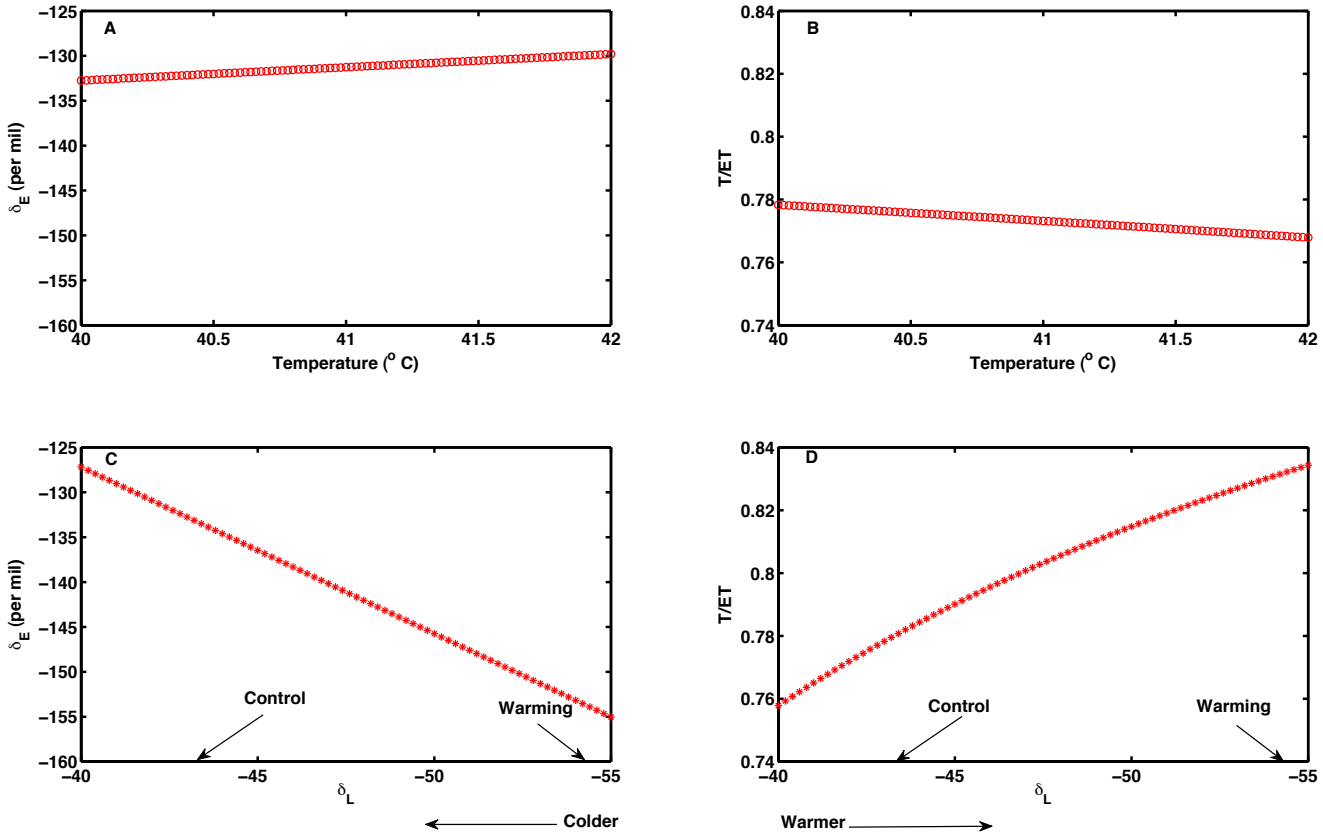
A
B
C
D
δE (per mil)
T/ET
Temperature (° C)
δL
Control
Warming
Colder
Warmer

Figure 9